NANO LETTERS

2007
Vol. 7, No. 3
663−667

Metal–Diboride Nanotubes as High-Capacity Hydrogen Storage Media

Sheng Meng,[†,‡,§] Efthimios Kaxiras,*[,§] and Zhenyu Zhang[‡,||]

Department of Physics, University of Texas, Austin, Texas 78712, Materials Science and Technology Division, Oak Ridge National Laboratory, Oak Ridge, Tennessee 37831, Department of Physics and Division of Engineering and Applied Sciences, Harvard University, Cambridge, Massachusetts 02138, Department of Physics and Astronomy, University of Tennessee, Knoxville, Tennessee 37996

Received November 17, 2006; Revised Manuscript Received February 7, 2007

ABSTRACT

We investigate the potential for hydrogen storage of a new class of nanomaterials, metal–diboride nanotubes. These materials have the merits of a high density of binding sites on the tubular surfaces without the adverse effects of metal clustering. Using the TiB_2 (8,0) and (5,5) nanotubes as prototype examples, we show through first-principles calculations that each Ti atom can host two intact H_2 units, leading to a retrievable hydrogen storage capacity of 5.5 wt %. Most strikingly, the binding energies fall in the desirable range of 0.2–0.6 eV per H_2 molecule, endowing these structures with the potential for room-temperature, near-ambient-pressure applications.

As one of the most abundant elements in the universe, hydrogen is receiving increasing attention as an attractive alternative to fossil fuels for clean energy.[1] However, a wealth of fundamental and technical challenges on hydrogen storage and transport, such as high gravimetric and volumetric density, low cost, and safety, must be overcome before a hydrogen fuel economy can be realized. Traditional methods to store hydrogen include using compressed gaseous or liquid H_2, which demands high pressure and/or low temperature, or using solids that adsorb H_2. Various systems have been proposed as potential storage media such as metal hydrides, carbon nanostructures, and porous materials.[1] For instance, $Ti(AlH_4)_4$, $Li_3Be_2H_7$, and Li_3N can store up to 9 wt % hydrogen, but these materials either do no exhibit reversibility or are reversible only at high temperatures (>520 K).[2] To date, the most promising materials performing near ambient conditions can only store up to 2.6 wt % H_2 at 10 bar and 313 K, using bulk TiV_2;[1] this is still far below the desired target of 6 wt % for practical automotive applications.[3]

In searching for an ideal H_2 storage medium operating at ambient conditions, several generic guidelines have been emphasized. First, the material should be light, usually consisting of first- or second-row elements only, and the active sites for molecular binding have to be dense in order to reach high storage capacity. Second, the material should have molecular binding energies in the range of 0.2−0.6 eV/H_2 for retrievable storage and fast kinetics at room temperature (RT), which *usually* corresponds to intact H_2 molecules binding. This requirement effectively rules out many materials. In particular, because H_2 is a relatively inert molecule, the storage materials must have active sites to achieve considerable H_2 binding strengths that are substantially stronger than van der Waals attraction.

Because of their large surface-to-weight ratios, nanotubes are attractive candidates for high-density hydrogen storage. However, most nanotubes are chemically inert and cannot bind molecules strongly. Earlier experiments reported considerable H_2 storage capacity of carbon-based nanomaterials, but the highest storage capacity demonstrated was only 0.43 wt % at RT after excluding experimental errors.[4] To overcome the inert nature of intrinsic nanotubes, one expects that significant improvements in H_2 storage capacity can be achieved for metal-doped nanotubes.[5−7] Indeed, it has been shown theoretically that a maximum retrievable H_2 storage density of 8.77 wt % with a binding energy of ∼0.3 eV/H_2 can be achieved on Sc-coated, B-doped fullerenes $C_{48}B_{12}$-$[ScH]_{12}$ [5] and a capacity of 7.69 wt % on Ti-coated carbon nanotubes (CNT).[6] However, formation of metal clusters can be energetically much more favorable than uniformly coated ions, as pointed out, for example, for the Ti-coated C_{60} system.[8] Such clustering, in turn, would substantially reduce the storage capacities of the hybrid nanomaterials from the maximal values.[8]

In this letter, we investigate a class of nanomaterials, metal−diboride nanotubes, as potential new media for

* Corresponding author. E-mail: kaxiras@cmt.harvard.edu.
† University of Texas.
‡ Oak Ridge National Laboratory.
§ Harvard University.
|| University of Tennessee.

10.1021/nl062692g CCC: $37.00
Published on Web 02/23/2007

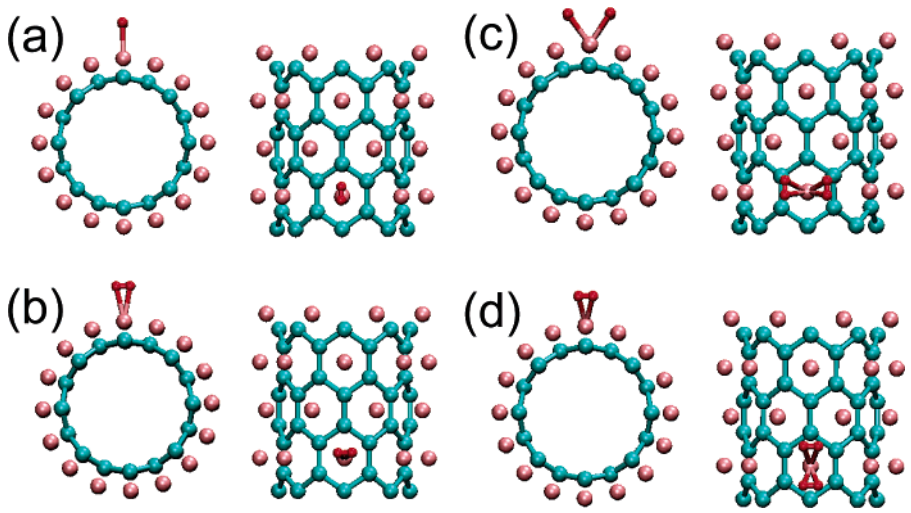

Figure 1. Atomic structures for single H_2 (a,b) and double H_2 (c,d) adsorption on a TiB_2 (8,0) nanotube. The H−H bond lies along the tube axis ("∥" configuration, a and c) or perpendicular to the axis ("⊥", b and d), shown in both top and side views.

hydrogen storage. Because the metal atoms are a natural part of the tubular structures, these materials have the merits of high-density binding sites on the tubular surfaces, inherently forbidding the tendency for metal clustering. Using TiB_2 (8,0) and (5,5) nanotubes as prototype examples, we show that each Ti atom can host two H_2 molecularly, leading to a retrievable H_2 storage capacity of 5.5 wt %. Most strikingly, the binding energies just fall in the desirable range of 0.2−0.6 eV per H_2, rendering them the potential for room-temperature, near-ambient-pressure applications. A detailed electronic structure analysis shows that the strong molecular binding stems from the resultant effect of local d−s orbital hybridization and intermolecular electrostatic attraction.

Our study is based on first-principles calculations in the framework of density functional theory. We use the VASP code[9] with ultrasoft pseudopotentials and employ both the local density approximation (LDA) and the PW91 generalized gradient approximation (GGA)[10] for the exchange correlation functional. It is well-known that GGA underestimates and LDA overestimates the binding energies,[7] so a comparison of the two approaches is useful for extracting reasonable results. We will generally quote only the GGA results and, wherever appropriate, we will also comment on the LDA results for comparison with experiment. In most cases, spin polarization is not required, as the metal−diboride nanotubes have zero magnetic moment; however, whenever unpaired H atoms are involved, spin-polarized calculations are employed to properly account for the magnetic moments of the unpaired electrons. The TiB_2 nanotubes are modeled in a supercell geometry, with dimensions 25 Å × 25 Å × $2L$ or 25 Å × 25 Å × L, where L is the unit length along the tube axis: for a (8,0) nanotube L = 5.5 Å, and for a (5,5) nanotube L = 6.3 Å. A plane wave cutoff of 260 eV and k-point sampling of 1 × 1 × 3 or 1 × 1 × 5 are used. Gaussian smearing width is 0.15 eV. All the atoms are allowed to relax until the forces have magnitudes less than 0.02 eV/Å.

Before adding H_2, we note that the bulk MB_2 compounds (M = Be, Mg, Ti, Sc, etc.) have been well established to be in the AlB_2 phase with intercalated layered structure. Here, the boron atoms form an *AA*-stacked graphitic network, with the metal atoms residing above the center of each hexagon.[11] The MB_2 compounds have interesting electronic and transport properties, as exemplified by the high superconducting transition temperature of MgB_2.[11] The naturally layered structure has also motivated extensive investigations using these materials as potential tubular archetypes.[12−15] In all of these studies, the M atoms were found essential in maintaining the charge neutrality and the honeycomb geometry of the B networks. This is captured by a simplified picture in which the ionized M^{2+} atoms stabilize the negatively charged B^- sheets.[14,16] Segregation of the M atoms is not possible because such a process would break the whole material. Our calculations show that it is at least 2.9 eV/Ti less stable if a Ti atom is removed from the B hexagonal centers and forms Ti clusters. This finding is qualitatively consistent with the result of Zhao et al., who showed that the introduction of B as dopants into C_{60} will substantially enhance the binding energy of Sc from 1.8 to 2.7 eV, thereby diminishing the clustering tendency of the Sc adatoms on the doped C_{60} surface.[5] Moreover, the M^{2+} ions serve as the active sites for molecular H_2 binding.

When H_2 is adsorbed on several MB_2 nanotubes and the isoelectronic LiBC nanotube,[16] different binding strengths are obtained. Specifically, BeB_2 and MgB_2 have H_2 binding energies (E_b) of about 0.03 eV, which is too small. On the other hand, TiB_2 and LiBC have significantly enhanced H_2 binding energy of 0.35 and 0.12 eV, respectively. In contrast, the binding energy of H_2 on a standard CNT, BN nanotube or B-doped CNT is much weaker (0.007, 0.002, and 0.013 eV, respectively). On ScB_2, the adsorption of the first H_2 is dissociative, giving the largest binding energy (1.63 eV) for this class of materials. Overall, TiB_2 has the most suitable E_b for retrievable H_2 storage. Accordingly, we primarily focus on this system below.

Figure 1 shows the optimized geometry of a single H_2 molecule (a,b) and two H_2 molecules (c,d) on a Ti atom of a TiB_2 (8,0) nanotube. The first H_2 molecule is adsorbed on

Table 1. Bond Lengths and Binding Energies Per Molecule for H_2 Adsorption on a TiB_2 (8,0) Nanotube in Different Coverage and Configurations [Parallel (∥) or Perpendicular (⊥)]

	$1H_2^{\parallel}$	$1H_2^{\perp}$	$2H_2^{\parallel}$	$2H_2^{\perp}$	1 ML$^{\parallel}$	1 ML$^{\perp}$	2 ML$^{\parallel}$	2 ML$^{\perp}$
d_{Ti-H} (Å)	2.06	2.05	2.02	1.97	2.07	2.06	2.01	2.04
d_{H-H} (Å)	0.79	0.79	0.81	0.83	0.79	0.79	0.83	0.82
E_b (eV)	0.35	0.34	0.14	0.20	0.33	0.33	0.20	0.09
E_b (eV)[a]	0.63	0.61	0.44	0.53	0.61	0.62	0.52	0.45

[a] LDA results.

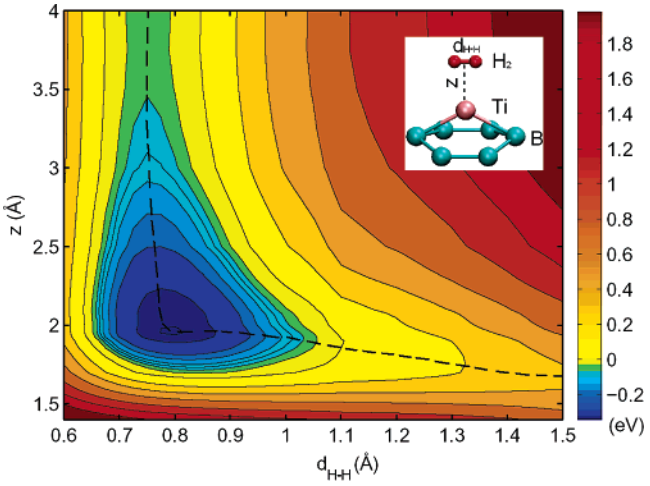

Figure 2. Contour plot of the potential energy surface for H_2 adsorption on a (8,0) TiB_2 nanotube. The dashed line indicates the minimum energy pathway for H_2 dissociation. The binding geometry is shown in the insert.

top of Ti, lying flat, with the H−H bond aligned either along or perpendicular to the nanotube axis, hereafter referred to as the "parallel" (∥) or "perpendicular" (⊥) configuration, respectively (Figure 1a and b). The two alignments have energies of 0.35 and 0.34 eV, with nearly identical Ti−H and H−H bond lengths of $d_{Ti-H} = 2.1$ Å and $d_{H-H} = 0.79$ Å (Table 1). Configurations with random H−H directions have energies in between, indicating that H_2 molecules can easily rotate along the azimuthal angle, with an energy barrier of 0.013 eV. In contrast, a single H_2 molecule with vertical H−H alignment automatically desorbs, indicating a repulsive interaction between the Ti and H_2 antibonding states.

A single H_2 molecule will not dissociate on the TiB_2 nanotube. The dissociated configuration, where two H atoms bind on the Ti bridge sites forming four Ti−H bonds, is 0.16 eV less stable than molecular adsorption and is likely prohibited by a large energy barrier. This is different from a Ti-coated CNT, where the first H_2 is dissociated with a large $E_b = 1.43$ eV,[6] but similar to the molecular H_2 adsorption on Be-doped fullerenes (BeC_{35}).[7] It is therefore interesting to explore the energetic landscape and the bonding nature of the molecular H_2 adsorption on TiB_2. Figure 2 illustrates the potential energy surface with respect to the H_2 adsorption height (z) and the H−H bond length (strength) upon H_2 adsorption. It shows clearly that H_2 can bind on the tube for a large range of $z = 1.7-4.0$ Å and $d_{H-H} = 0.65-1.05$ Å (the negative energy region). Pushing H_2 closer to Ti results in a sharp energy increase and a dramatic elongation of the H−H bond, and finally splits the H_2 molecule at $z = 1.6$ Å due to large charge overlap. The binding region extends to $z > 4$ Å despite the small E_b, indicating that the H_2 molecule is attracted by the long-range electric field of Ti^{2+} beyond this point ($z = 4.0$ Å). Similar results have been found in $Ni^{+}-6H_2$.[17] A detailed analysis reveals that Ti binds H_2 through the Dewar mechanism[18] to form Kubas metal−dihydrogen complexes,[19] with 0.1 electrons transferred from Ti to H_2.

The binding of two H_2 molecules to the same Ti atom is shown in Figure 1c and d. Here, both of the adsorbed H_2 molecules have been displaced from the top site by 1.1 Å. The Ti−H bonds are shortened and the H−H bonds elongated, compared to the case of single H_2 adsorption (Table 1). The corresponding adsorption energies are roughly one-half of that for a single H_2, and the perpendicular $2H_2$ adsorption configuration is 0.06 eV/H_2 more favorable than the parallel one. This is due to intersite electrostatic attraction between a H_2 molecule and a neighboring Ti: In the perpendicular configuration, each H_2 has two neighboring Ti ions located only 3.0 Å away on the Ti rings around the tube axis, while in the parallel configuration, each H_2 has only 1 Ti ion 3.9 Å away on one side. The counting is based on the observation that a neighboring Ti only moderately attracts a H_2 molecule when the Ti−H−H complex forms a planar geometry (roughly an equilateral triangle) but repels a H_2 molecule when the Ti−H−H complex forms a collinear geometry, as in the case of the first H_2 adsorption.

We have also carried out detailed calculations to show that, when a third H_2 molecule is adsorbed to the same Ti site, the molecule will be repelled to a neighboring unoccupied Ti. Furthermore, as the coverage increases further, the H_2 molecules can reach a uniform monolayer (ML) configuration on the TiB_2 nanotube. Here 1 ML is defined by the condition that every TiB_2 unit in the tube is occupied by a single H_2 molecule. Each H_2 in the monolayer geometry resembles the case of the first H_2 adsorption, with a similar binding strength of 0.33 eV.

Interesting results are achieved for 2 ML adsorption, where each Ti binds two H_2 molecules. The parallel configuration forms a sunflower-like geometry (Figure 3a) and has a large E_b of 0.20 eV/H_2, higher by 0.06 eV (∼30%) than that for single $2H_2-Ti$ adsorption. This enhancement stems from the fact that the $2H_2-Ti$ units in a ring around the tube axis polarize each other and facilitate significant intersite attraction. In contrast, the energy for the perpendicular configuration is reduced to as small a value as 0.09 eV. This reduction is caused by the lack of attractive neighboring Ti ions, as well as the presence of strong inter-H_2 repulsion between nearest rings. We also note that a ring of perpendicular $2H_2$ is not favorable because of the strong intersite repulsion. According to the 18-electron rule,[5] each Ti in the TiB_2 tube could bind a maximum of 5 H_2 molecules (there are six π-electrons from the negatively charged B^- sheet coordinated with each Ti atom, and two valence electrons left in Ti; to form a closed shell, each Ti needs 10 more electrons). Nevertheless, for the system studied here, the concentration of H is much lower than that required by this

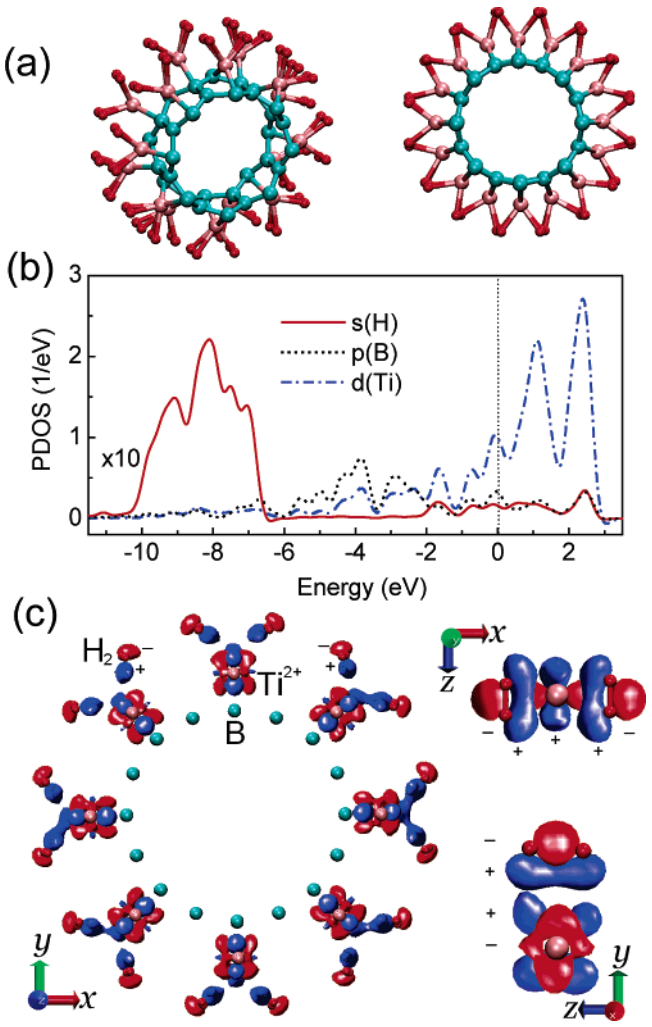

Figure 3. (a) Relaxed geometry of 2 ML H_2 adsorption on a (8,0) TiB_2 nanotube. The H−H bonds are parallel to the tube axis. (b) PDOS contributed from a unit of TiB_2 and adsorbed H_2, containing 4 H, 1 Ti, and 2 B atoms. (c) Isodensity surface of the charge difference between the total system and that for well-separated nanotube and hydrogen subsystems, at levels of ±0.05 e/Å.^{3} Electron accumulation/depletion regions are shown in blue(+)/red-(−). For clarity, only isosurfaces around a Ti atom are shown in the panels on the right.

rule because of the steric repulsion among the H_2 units in the dense adlayer and the sharing of electrons from H_2 units adsorbed on neighboring Ti atoms within a distance of 3.0−3.3 Å from the Ti atom at focus.

To elucidate the physical origin for the above observations, we plot in Figure 3b,c the projected density of states (PDOS) and the charge density difference upon adsorption of 2 ML H_2 on a TiB_2 nanotube. The TiB_2 nanotube is metallic, with dominant Ti *d* states at the Fermi energy (zero), in agreement with many calculations of MB_2 nanotubes,[12−14] although Guerini and Piquini predicted TiB_2 (6,0) to be a semiconductor.[15] These states are responsible for broadening the H−H bonding states from −11 to −6 eV and weakly perturb the antibonding states around the Fermi level. From the charge density plot, we clearly see that a Ti atom interacts with the s orbitals of adsorbed H_2 through the d_{xy} and d_{yz} states, producing electron depletion (accumulation) of d_{xy} (d_{yz}). As a result, the H_2 molecule is polarized, with electron gain on the side near Ti and electron loss on the side away from Ti, resulting in a net charge excess of 0.15*e*. The charge-transfer facilitates intersite attraction between a negatively charged H_2 and the neighboring cations $Ti^{2.3+}$; this attraction, in turn, accounts for 30−40% of the binding energy to maintain the high-density H_2 monolayers.

In addition to its appealing geometry, the 2 ML H_2 configuration on a TiB_2 nanotube is also highly desirable for practical purposes, as it stores 5.5 wt % H_2. The calculated GGA binding energy is ∼0.2 eV/H_2, thereby favoring RT, near-ambient-pressure operations without metal clustering. Using the LDA results (Table 1), this estimate is raised to ∼0.6 eV for single H_2 and ∼0.5 eV for 2 ML; an intermediate value between the GGA and LDA results is most likely closer to the binding energies from experiment and quantum Monte Carlo simulations.[7] Furthermore, our molecular dynamics (MD) simulations at RT show that a TiB_2 (8,0) nanotube can hold six more H_2 per unit length inside the tube, further increasing the capacity to 6.5%. For comparison, we also studied the adsorption energetics of fully H_2-saturated ScB_2 (8,0). A unit length of the ScB_2 tube (16 ScB_2 units) could adsorb a maximum of 32 H_2 molecules. Eight of them are found to adsorb dissociatively, forming covalent Sc−H bonds, with an average adsorption energy of 1.43 eV/H_2; the remaining H_2 adsorb molecularly, with an average binding energy of 0.12 eV/H_2, giving a reversible H_2 storage capacity of 4.3 wt %.

At this point, it is worthwhile to address various issues that may prove critical in experimental realization of the TiB_2 nanotubes for high-density H storage: (i) Various MB_2 nanotubes have been predicted to be stable in a number of previous studies.[12−14] In particular, the cohesive energy is 6.0 eV for a TiB_2 (8,0) nanotube per atom. Furthermore, compared with the curvature energy cost of CNT (0.15 eV), the low curvature energy cost (0.04 eV) makes a TiB_2 tube[15] energetically accessible, possibly by template synthesis or film convolution, as discussed in ref 14.

(ii) Ti does not bind at the inner B wall of a TiB_2(8,0) nanotube. Instead, if one or more Ti atoms were placed at the inner wall, the Ti−B network would break. Our calculations using larger nanotubes such as TiB_2 (11,11) show that the Ti-outside configuration is 0.10 eV/atom more stable than the Ti-inside configuration. This contradicts the conclusion of ref 14, where the Ti-inside configuration is predicted to be more stable. We attribute the difference in stability to the different interactions used in the two studies, namely, the empirical tight binding method in the earlier study versus the more accurate first-principles method in the present case.

(iii) Once formed, a TiB_2 nanotube is rather stable. Our MD simulations show that the (8,0) tube is stable up to >1000 K.

(iv) The strong binding between nanostructures could reduce the optimal H_2 storage capacity because they form into clusters and bundles.[20] But the attraction between two TiB_2 (8,0) nanotubes is weak, only 0.027 eV/atom at the nearest Ti−Ti distance of 3.0 Å. This makes it easy to have well-separated TiB_2 nanotubes for H_2 storage. Interestingly,

this is not the case for the AlB_2 nanotube. Quandt et al. predicted the most stable structure of AlB_2 (6,6) *nanotube bundles*, which have Al both inside the tube and between the B walls, forming strong Al−B bonds. This agrees with our finding that a *single* AlB_2 tube is not stable (Al segregates).

(v) During and/or after its synthesis, it is inevitable that the TiB_2 nanotubes will interact with residual gases in the chamber, a process that might passivate the nanotubes before H_2 are introduced into the system. We calculated the interaction of TiB_2 (8,0) with the likely common gases in an experimental setting and found that the binding strength is medium. Specifically, the binding energy with a H_2O molecule and an (OH + H) group is 0.82 and 2.22 eV, respectively, while that for CO is 1.43 eV. Therefore, these molecules can be removed at relatively low temperatures.

(vi) Finally, we have carried out detailed MD simulations to show that indeed H_2 desorbs intact during heating.

Before closing, we note that other types of TiB_2 nanotubes would have the same optimal hydrogen storage capacity as the (8,0) tube. For instance, a (5,5) TiB_2 nanotube can bind H_2 molecules strongly, with a binding energy of 0.47 eV (∥) and 0.30 eV (⊥) for single H_2, and 0.24 eV/H_2 for 2 ML adsorption (∥). The capacity might increase if the radius of the nanotube changes, allowing more H_2 molecules to bind at the interstitial sites through long-ranged electrostatic attraction. Moreover, our detailed calculations show that even a freestanding planar layer of TiB_2 can have appealing properties for H_2 storage. Here, the first layer of H_2 dissociates, with an adsorption energy of 0.743 eV/H_2; the second layer of H_2 adsorbs as intact molecules, with a binding energy of about 0.17 eV/H_2. The dissociated H atoms also facilitate peeling off more freestanding TiB_2 layers from the TiB_2(0001) surface, as indicated in experiment.[21] In contrast, a H atom in bulk TiB_2 has a binding energy of 0.7 eV (with reference to a free H atom) and is not stable. Considering the binding energy of 4.5 eV in a H_2 molecule, it requires at least $4.5-0.7 \times 2 = 3.1$ eV to split a H_2 and store it inside bulk TiB_2.

In conclusion, we have found that metal−diboride nanotubes and related nanomaterials have the merit of dense sites for molecular hydrogen adsorption without the adverse effect of metal clustering. Together, the predicted H_2 storage capacity of 5.5 wt % and the desirable binding energies of 0.2−0.6 eV/H_2 make these materials appealing candidates for room-temperature, near-ambient-pressure applications. We have also examined the various issues that might be encountered in experimental realization of these intriguing predictions.

Acknowledgment. This work has been supported by the U.S. NSF (grant nos. DMR-0306239, DMR-0606485, and DMR-0325218) and the U.S. DOE (grant no. DEFG02-05ER46209, and the Division of Materials Sciences and Engineering, Office of Basic Energy Sciences, DOE, under contract DE-AC05-00OR22725 with Oak Ridge National Laboratory, managed by UT-Battelle, LLC). The calculations were performed at ORNL's Center for Computational Sciences.

References

(1) Schlapbach, L.; Züttel, A. *Nature* **2001**, *414*, 353.
(2) Chen, P.; Xiong, Z. T.; Luo, J. Z.; Lin, J. Y.; Tan, K. L. *Nature* **2002**, *420*, 302.
(3) http://www1.eere.energy.gov/hydrogenandfuelcells/mypp/.
(4) Kajiura, H.; Tsutsui, S.; Kadono, K.; Kakuta, M.; Ata, M.; Murakami, Y. *Appl. Phys. Lett.* **2003**, *82*, 1105.
(5) Zhao, Y. F.; Kim, Y. H.; Dillon, A. C.; Heben, M. J.; Zhang, S. B. *Phys. Rev. Lett.* **2005**, *94*, 155504.
(6) Yildirim, T.; Ciraci, S. *Phys. Rev. Lett.* **2005**, *94*, 175501.
(7) Kim, Y. H.; Zhao, Y. F.; Williamson, A.; Heben, M. J.; Zhang, S. B. *Phys. Rev. Lett.* **2006**, *96*, 016102.
(8) Sun, Q.; Wang, Q.; Jena, P.; Kawazoe, Y. *J. Am. Chem. Soc.* **2005**, *127*, 14582.
(9) Kresse, G.; Hafner, J. *Phys. Rev. B* **1993**, *47*, 558.
(10) Perdew, J. P.; Chevary, J. A.; Vosko, S. H.; Jackson, K. A.; Pederson, M. R.; Singh, D. J.; Fiolhais, C. *Phys. Rev. B* **1992**, *46*, 6671.
(11) Nagamatsu, J.; Nakagawa, N.; Muranaka, T.; Zenitani, Y.; Akimitsu, J. *Nature* **2001**, *410*, 63.
(12) Quandt, A.; Liu, A. Y.; Boustani, I. *Phys. Rev. B* **2001**, *64*, 125422.
(13) Zhang, P.; Crespi, V. H. *Phys. Rev. Lett.* **2002**, *89*, 056403.
(14) Ivanovskaya, V.; Enjashin, A. N.; Sofronov, A. A.; Makurin, Y. N.; Medvedeva, N. I.; Ivanovskii, A. L. *J. Mol. Struct. (THEOCHEM)* **2003**, *625*, 9.
(15) Guerini, S.; Piquini, P. *Microelectron. J.* **2003**, *34*, 495.
(16) Ponomarenko, O.; Radny, M. W.; Smith, P. V.; Seifert, G. *Phys. Rev. B* **2003**, *67*, 125401.
(17) Niu, J.; Rao, B. K.; Jena, P. *Phys. Rev. Lett.* **1992**, *68*, 2277.
(18) Michael, D.; Mingos, P. *J. Organomet. Chem.* **2001**, *635*, 7.
(19) Kubas, G. J. *J. Organomet. Chem.* **2001**, *635*, 37.
(20) Sun, Q.; Jena, P.; Wang, Q.; Marquez, M. *J. Am. Chem. Soc.* **2006**, *128*, 9741.
(21) Zhang, D. M.; Fu, Z. Y.; Guo, J. K. *Key Eng. Mater.* **2003**, *249*, 119.

NL062692G